ACS Catalysis

Letter

pubs.acs.org/acscatalysis

Challenging the Major/Minor Concept in Rh-Catalyzed Asymmetric Hydrogenation

Ilya D. Gridnev*,† and Tsuneo Imamoto*,‡,§

†Department of Chemistry, Graduate School of Science, Tohoku University, Sendai 980-8578, Japan

‡Department of Chemistry, Graduate School of Science, Chiba University, Chiba 263-8522, Japan

§Research and Development Division, Nippon Chemical Industrial Co., Ltd., Tokyo 136-8515, Japan

Supporting Information

ABSTRACT: Herein, we provide evidence showing that the long-held major−minor concept for catalytic asymmetric reactions needs to be readdressed. The asymmetric hydrogenation of enamide **1** catalyzed by the chiral Rh(I) complex of (*R*,*R*)-BenzP* quantitatively yields the corresponding hydrogenated *R*-product **2** with 89.6% ee. The most abundant catalyst−substrate species in the reaction pool was found to be [Rh((*R*,*R*)-BenzP*)(Ph(MeCONH)C═CH_2)]$^+SbF_6^-$ (**5**). This species is also the most reactive to hydrogen among the various Rh complexes. Low-temperature hydrogenation experiments showed direct transformation of **5** to **2** with over 98% ee (*R*). However, the oxidative addition of H_2 to **5** would yield the *S*-product. Computation has now revealed a low-energy *R*-enantioselective route, whereby H_2 addition to **5** is followed by π-bond dissociation, isomerization of nonchelating Rh species, and recoordination of the double bond before C−H bond formation occurs.

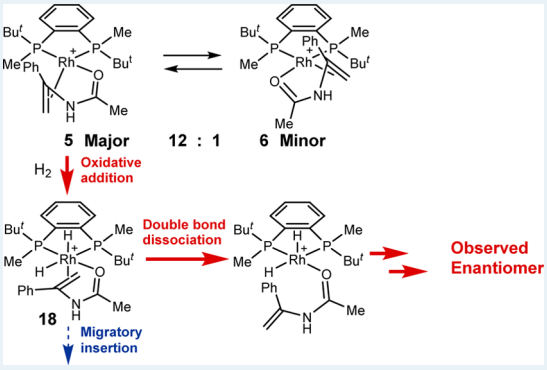

KEYWORDS: *asymmetric hydrogenation, Rh complexes, origin of enantioselectivity, DFT calculations, reaction mechanism*

The origin of enantioselectivity in catalytic asymmetric reactions is an actively explored area of broad interest and importance.[1] Clear understanding of the intrinsic mechanisms responsible for the extremely high orders of enantioselection observed in some of these reactions is essential for the further development of highly efficient methods for the synthesis of chiral drugs and other fine chemicals.

Rh-catalyzed asymmetric hydrogenation is one of the most mechanistically studied catalytic asymmetric reactions. Extremely high optical yields up to almost 100% make these studies relevant to reliable conclusions, and high solubility of the catalysts and intermediates facilitates NMR studies.

The early mechanistic conclusion derived from these studies was the famous major/minor concept that connected the relative abundance of the diastereomeric catalyst−substrate complexes with their reactivity toward H_2 in the oxidative addition reaction.[2−4] Although there were no attempts to rationalize the frequently observed high reactivity of less abundant species until the computational work of Landis et al.,[5−9] the simplicity and educative attractiveness of the major/minor concept made it widespread and popular not only in the research papers but also in the textbooks and lecture courses.

However, further mechanistic studies showed that the major/minor concept is unlikely to be universally acceptable for the explanation of the origin of enantioselection in the Rh-catalyzed asymmetric hydrogenation. The feasibility of another, "dihydride" pathway was demonstrated in numerous catalytic systems.[10−16] Moreover, it has been shown that the enantiodetermining step in all known catalytic systems takes place in the octahedral Rh(III) complexes, rather than in square planar Rh(I) complexes. Hence, the chirality induction must take place after the hydrogen activation, and the oxidative addition to the catalyst−substrate complexes is unlikely a stereoregulating step.[17]

Recently, we have computed several catalytic cycles of Rh-catalyzed asymmetric hydrogenation with BenzP*, TangPHOS, and TrichikenfootPHOS ligands.[18−20] In all these cases, it has been shown that the activation of hydrogen is likely to proceed through the species with uncoordinated double bond.

Furthermore, Evans[21] and Heller[22] have reported the cases when the structures of the "major" catalyst−substrate complexes corresponded to the handedness of the product, and we have recently reported that almost perfect optical yields are obtained in a system where no substrate binding is observed even at −100 °C.[20] These findings clearly indicate that the relative abundance of the Rh(I) square planar complexes does not stand in any relationship with the sense and level of enantioselection.

Received: February 26, 2015
Revised: April 6, 2015
Published: April 6, 2015

DOI: 10.1021/acscatal.5b00424
ACS Catal. 2015, 5, 2911−2915

Here we report a combined NMR and computational study of the mechanism of asymmetric hydrogenation of enamide **1** catalyzed by Rh complex of (*R*,*R*)-BenzP*.[18] The "major" catalyst−substrate complex (**5**) formed in the reaction pool was found to be the most reactive species toward H_2 among all conceivable intermediates. Experimentally, in two independent experiments, we have observed its rapid reaction with H_2 at −78 °C, accompanied by accumulation of the reaction product with over 98% ee (*R*). However, because the substrate was *re*-coordinated in **5**, *the stereoinduction did not take place in the oxidative addition step*.

Therefore, relatively rapid hydrogenation of "minor" catalyst−substrate complex in the initial experiments, which led to the formulation of the major/minor concept,[2−4] was not a solid reason to conclude that it was a direct origin of the enantioselectivity. Even though the configuration of the product was the expected one, this could be a coincidence that could happen with quite high probability (50%).

Detailed computations of the catalytic cycle confirmed these conclusions and gave an accurate prediction of the sense and level of enantioselection in this reaction.

Asymmetric hydrogenation of enamide **1** catalyzed by Rh complex of (*R*,*R*)-BenzP* quantitatively yields the corresponding hydrogenation product **2** with 89.6% ee (*R*) (Scheme 1).

Scheme 1. Catalytic Asymmetric Hydrogenation of Enamide 1

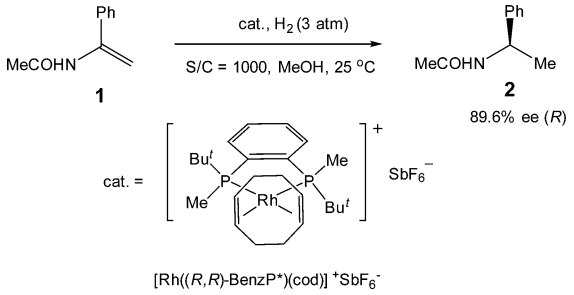

Analyzing the detailed data shown in Table 1, one can conclude that although the optical yields are not sensitive to the hydrogen pressure, there is notable dependence of the ee's on the nature of the solvent. The higher ee's were observed for the polar solvents like 2-propanol and ethyl acetate, whereas use of less polar solvents like THF or dichloromethane led to decrease of enantioselectivity.

The temperature dependence of the optical yields has a regular character, as can be seen from the corresponding plot of the ln(*R*/*S*) versus reciprocal temperature (see SI, Figure S1) that demonstrated linear dependence (R^2 = 0.984). These data suggest that most probably the observed optical yields arise from the competition of only two pathways leading to the corresponding *R* and *S* products, because otherwise much more complicated temperature dependence would be expected.[1b]

For the experimental mechanistic studies, we have used a norbornadiene complex of BenzP* (**3**) as a catalytic precursor because norbornadiene is hydrogenated off much faster than cyclooctadiene, which leads to cleaner samples. Addition of 2 equiv of **1** to a solution of the solvate complex **4** gave an equilibrium mixture of two chelate complexes **5** and **6** in a ratio of 12:1. The structures of **5** and **6** were elucidated from the NMR data. All signals in the NMR spectra of **5** and **6** were unambiguously assigned using routine 2D NMR techniques.

Table 1. Dependence of the Optical Yields Observed in the Asymmetric Hydrogenation of 1 Catalyzed by the (*R*,*R*)-BenzP*-Rh Complex on the Temperature, Pressure, and Solvent[a]

solvent	pressure (atm)	temperature (K)	substrate−catalyst ratio (S/C)	time (h)	ee (%)[b]
MeOH	3	323	1000	1	85.7
	3	298	1000	1	89.6
	3	273	1000	5	93.3
	3	248	100	5	96.1
	3	223	50	24[c]	97.0
	2	195	2	0.3[d]	98.9
	1	298	1000	24	88.2
	30	298	1000	1	89.4
	50	298	1000	1	88.2
	70	298	1000	1	87.8
i-PrOH	3	298	1000	1	90.0
ethyl acetate	3	298	1000	1	94.9
THF	3	298	1000	1	84.9
CH_2Cl_2	3	298	1000	1	82.8

[a]Conversion was 100% unless specified otherwise. [b]The enantiomeric excesses were determined by GC analysis. *N*-Acetyl-1-phenylethylamine: Varian Chirasil-DEX CB, 120 °C, isothermal, 1.1 mL/min, (*S*) t_1 = 23.8 min, (*R*) t_2 = 25.7 min. [c]Conversion 64%. [d]Low-temperature NMR experiment.

The *re*-coordination of the substrate in the major complex **5** was unambiguously assigned from NMR data. The ROE's observed in the phase-sensitive 2D ROESY spectrum (Figure S7) unequivocally define **5** as a complex containing *re*-coordinated substrate, and **6** with *si-gaushe* coordination. This conclusion is strongly supported by characteristic high-field shielding of the protons of Bu^t group in **5** and Me group in **6** under influence of the adjacent phenyl ring (Figure 1).[11] Computational data (Scheme 2) are also in accord with the above assignment.

The exchange cross-peaks in the 2D ^{1}H−^{1}H ROESY spectrum taken at −20 °C provided evidence for an intermolecular exchange between **5** and **6**. On the other hand, the only exchange cross-peaks observed in the 2D ^{1}H−^{1}H ROESY spectrum taken at −80 °C were due to the hindered rotation of the phenyl group of the coordinated substrate in **5**. Thus, **5** and **6** are not interconverting at this temperature.

To find the pathway for the hydrogen activation in the catalytic cycle, we have computed six possible scenarios (Scheme 3). Hydrogen could be activated via oxidative addition to the catalyst **4** via barrierless formation of molecular hydrogen complex **8**; the following oxidative addition could give diastereomeric dihydrides **9** and **10** via **TS1** and **TS2**, respectively, with relative free energies of 13.4 and 13.0 kcal mol^{-1}.

Otherwise, the catalyst could be initially activated via coordination of the carbonyl group of the substrate yielding nonchelating square planar complexes **11** or **12**. The TS's of oxidative addition to these complexes (**TS3**, 6.8 kcal mol^{-1} and **TS4**, 7.6 kcal mol^{-1}) are significantly more stable than **TS1** and **TS2** (Scheme 3). Moreover, **TS3** and **TS4** are more stable than **TS6** and **TS7**, the transition states of the oxidative addition in chelate complexes **6** and **7** with *si*-coordinated double bond. Nevertheless, the most facile oxidative addition **TS5**, 4.2 kcal

DOI: 10.1021/acscatal.5b00424
ACS Catal. 2015, 5, 2911−2915

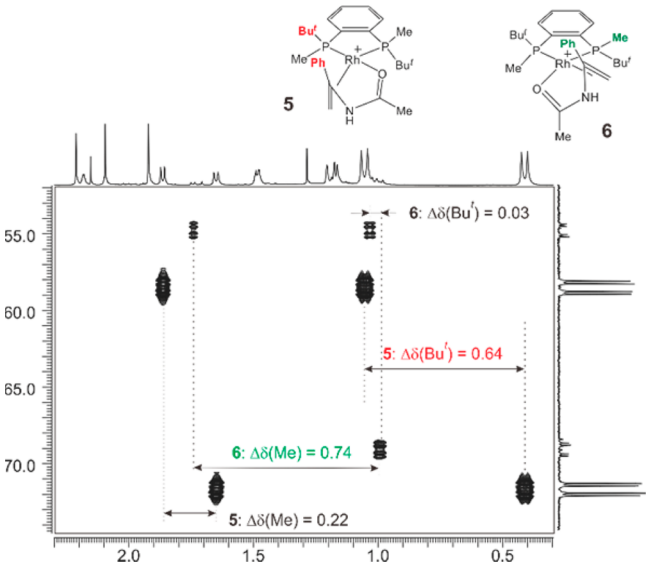

Figure 1. ^{1}H−^{31}P HMBC NMR spectrum (600 MHz, CD_3OD,-60 °C) of the equilibrium mixture of catalyst−substrate complexes **5** and **6** (section plot). Shielding of one of the *t*-butyl groups in **5** and one of the methyl groups in **6** defines the mode of the double bond coordination in both complexes.

Scheme 2. Formation and Relative Stabilities of the Catalyst−Substrate Complexes 5−7

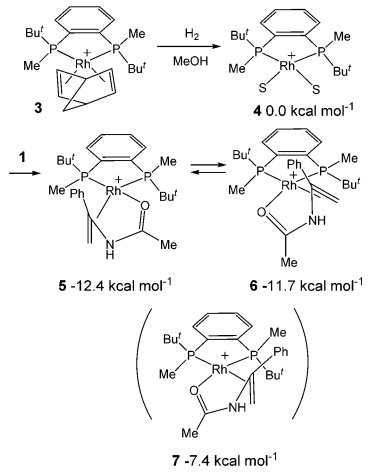

mol^{-1}, was computed for the chelate complex **5** with *re*-coordinated double bond (Figure 2).

We concluded therefore that in the catalytic cycle involving the catalyst **4** and the substrate **1** the activation of hydrogen proceeds directly via oxidative addition to the major component of the reaction pool, chelate complex **5**.

To check this conclusion experimentally, we monitored the hydrogenation of the sample prepared by the addition of 2-fold excess of **1** to a solution of **4** in deuteriomethanol at −78 °C. Figure 3 shows that at the initial stage of the reaction hydrogenation of the sample led to significant decrease of the concentration of **5**, whereas the concentration of **6** remained practically unchanged. Similar observations were made for another sample prepared by the addition of 4-fold excess of **1** to a solution of **4** at −78 °C (see SI, Figure S2). The ee's of the reaction product obtained after quenching of the samples were 98.9% and 98.1% (*R*), respectively. It should be noted that these ee values nicely fit the regular dependence of ee on the

Scheme 3. Different Pathways for Hydrogen Activation Computed on the WB97XD/SDD(Rh)/6-31-G(All Others)/SMD(Methanol) Level of Theory[a]**

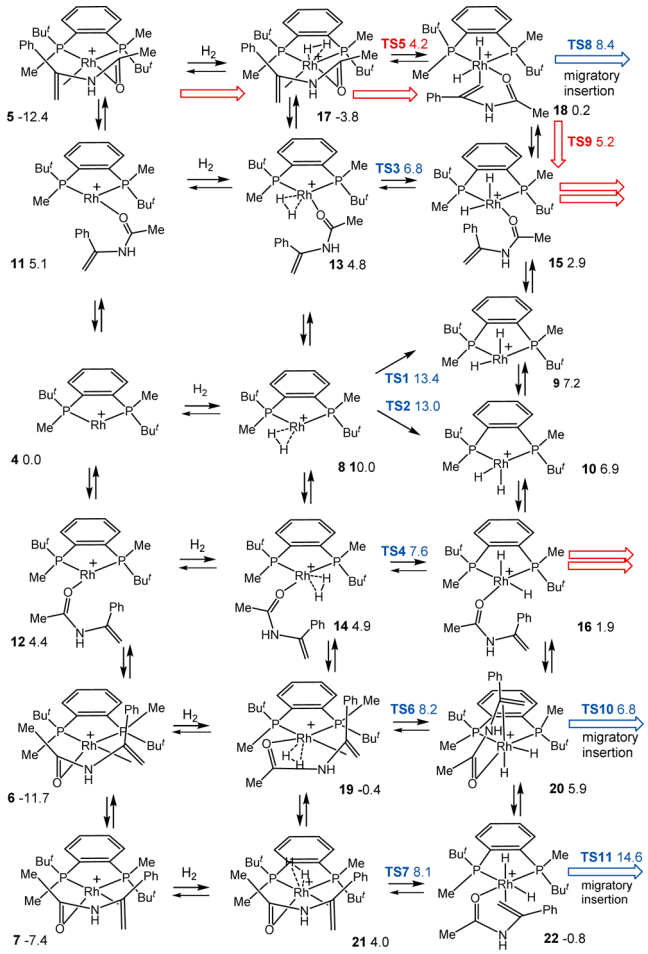

[a]Relative Gibbs free energies are shown in kcal mol^{-1} relative to 4 + 1 + H_2. The lowest energy pathways are shown in red.

temperature, confirming the uniform mechanism in a broad temperature range.

Because the substrate was *re*-coordinated in **5**, whereas the *R*-product was obtained almost exclusively, we concluded that the oxidative addition of H_2 to **5** must be followed by the dissociation of the double bond. Indeed, we have found that the corresponding **TS9**, 5.2 kcal mol^{-1} is 3.2 kcal mol^{-1} more stable than the transition state **TS8** for the migratory insertion in the dihydride intermediate **18** generated via the oxidative addition to the catalyst-substrate complex **5**.

In other words, after the hydrogen is activated via the oxidative addition to **5**, the migratory insertion does not take place immediately, because dissociation of the double bond proceeds much faster. This dissociation yields the nonchelating dihydride complexes **15** and **16** with different configuration at the Rh atom.

These complexes interconvert with low activation barrier via molecular hydrogen complexes **13** and **14**, which differ only slightly by the orientation of the molecule of H_2 (Scheme 4).

The complex with *si*-coordinated double bond **6** is likely to be hydrogenated via **16** because this route provides a lower activation barrier compared to the direct oxidative addition.

DOI: 10.1021/acscatal.5b00424
ACS Catal. 2015, 5, 2911−2915

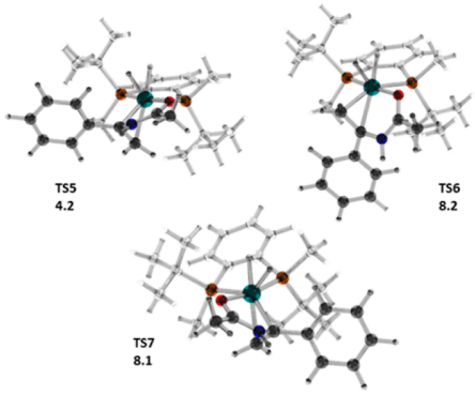

Figure 2. Optimized structures and relative free energies (298 K, kcal mol^{-1} relative to **4** + **1** + H_2) of transition states for the oxidative addition of H_2 to complexes **5** (up), **6** (middle), and **7** (below). The relative stabilities of these transition states are well understood by analyzing their structures. In the case of **TS5** the unsubstituted $=CH_2$ group moves to the bottom face of the chelate cycle without meeting any considerable hindrance. In the case of **TS6**, it is the $=$CPh(NHAc) group, which must move to the same direction, and the chelate cycle Rh−C−NH−C(Me)−O−Rh must overcome close contacts with the Bu^t group. The case of **TS7** is similar to **TS5**, but it is significantly less stable due to the close contacts between the phenyl substituent and the Bu^t group of the catalyst. Computations were done on the WB97XD/SDD(Rh)/6-31-G**(all others)/SMD-(Methanol) level of theory.

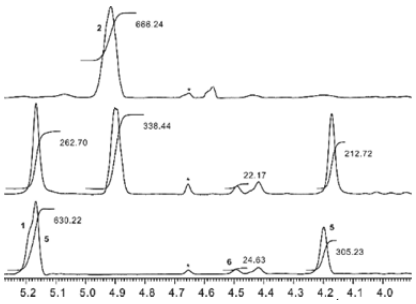

Figure 3. Section plots of ^1H NMR spectra (500 MHz, CD_3OD, −80 °C, [Rh] = 3.8 × 10^{-2} mol L^{-1}). Bottom: spectrum of the sample obtained by adding 2 equiv of **1** to a CD_3OD solution of the catalyst **4**. Middle: spectrum of the same sample after admitting H_2 at −78 °C and 4 min hydrogenation at the same temperature. Upper: spectrum of the same sample after additional 10 min hydrogenation at −78 °C. Spectra were integrated using the signal of the remaining protons of the solvent as a reference with the assigned intensity 1000. Asterisks indicate the signal of an impurity. Approximately two turnovers were performed.

Scheme 4. Interconversion of Non-Chelating Octahedral Complexes 15 and 16

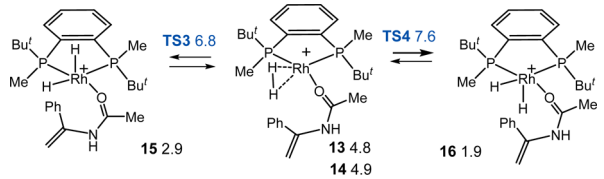

Thus, although the exact pathway for the hydrogen activation is different from the previously studied cases,[18−20] it results in the same reaction pool containing *nonchelating* octahedral dihydrides as would be obtained by the hydrogen activation via dihydride or semidihydride pathways involving oxidative addition to the complexes **4**, **11** or **12**.

Hence, similarly to the previously studied cases,[18−20] the fastest secondary coordination of the double bond in the octahedral Rh(III) complex followed by migratory insertion will determine the configuration of the product. Formation of four different dihydride complexes **23**−**26** with the double bond coordinated at the equatorial coordination site of the rhodium atom coplanar to the P−Rh—H^{trans} unit (Scheme 5) was

Scheme 5. Different Pathways for Hydrogen Activation Computed on the WB97XD/SDD(Rh)/6-31-G(All Others)/SMD(Methanol) Level of Theory[a]**

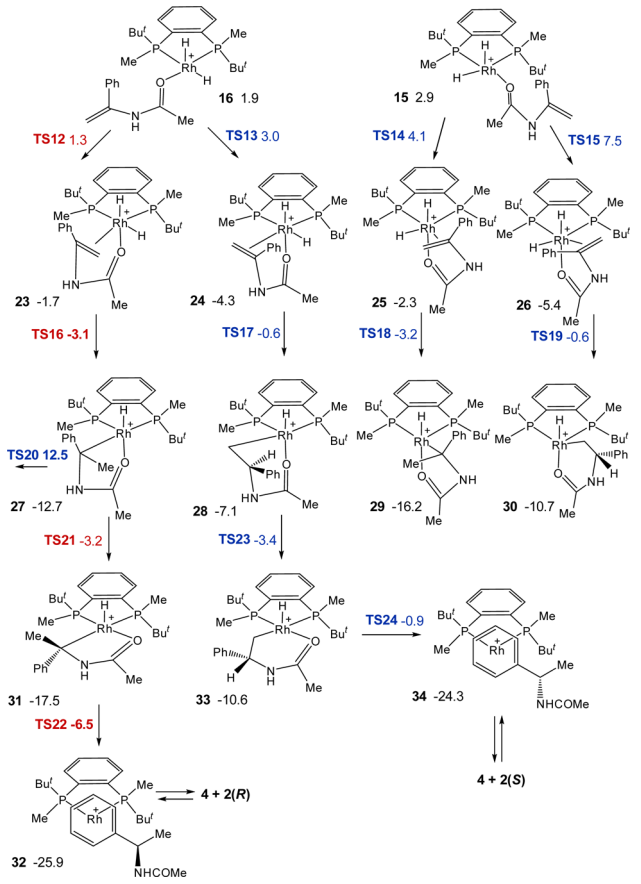

[a]Relative Gibbs free energies are shown in kcal mol^{-1} relative to 4 + 1 + H_2. The lowest energy pathways are shown in red.

analyzed by approaching a corresponding carbon atom (α or β) of the carbon−carbon double bond in complexes **15** and **16** to the free coordination site. As a result, the corresponding TS's **TS12**−**TS15** were located (Scheme 5).

Migratory insertion in either of the dihydride intermediates **23**−**26** is extremely facile, as is seen from the relative energies of **TS16**-**TS19** (Note also that **TS16**−**TS19** are 9.0−17.8 kcal mol^{-1} more stable than **TS8**, **TS10**, **TS11**). Hence, the optical yield of the product must reflect the competition between the different modes of the double bond coordination, i.e., by the difference in the relative free energies of the **TS12**−**TS15**. The most stable among them is **TS12**, 1.3 kcal mol^{-1} corresponding to the α-*R* pathway. The next in stability is **TS13**, 3.0 kcal mol^{-1} corresponding to the β-*S*-pathway. Because **TS14** and **TS15** are still less stable, one can neglect the contribution from the corresponding α-*S* and β-*R*-pathways coming to the

DOI: 10.1021/acscatal.5b00424
ACS Catal. 2015, 5, 2911−2915

conclusion that the optical yield is defined via the difference in stabilities of **TS12** and **TS13**, 1.7 kcal mol^{-1}. This calculated value correlates closely to the experimentally determined value of 1.74 kcal mol^{-1} (vide supra). Given the judicious modeling of a complex system, such a level of agreement demonstrates the virtue of DFT computations in predicting the sense and level of enantioselection.[23]

The TS's for the reductive elimination from the monohydride **27** was computed to be too high in energy (**TS20**, 12.5 kcal mol^{-1}), but it can easily rearrange into **31** (**TS21**, −3.2 kcal mol^{-1}), which readily eliminates the product via **TS22**, −6.5 kcal mol^{-1}). Similarly in the β-*S*-pathway, the reductive elimination proceeds via the rearrangement of **28** to **33** (Scheme 5). Similar rearrangements of monohydride intermediates were previously described.[10,13,14]

In conclusion, we have discovered an example of a catalytic asymmetric hydrogenation reaction in which activation of H_2 via oxidative addition to a chelate catalyst−substrate complex is followed by the dissociation of the carbon−carbon double bond. This means that experimental observation of a relatively fast reaction of H_2 with some catalyst−substrate complex does not necessarily mean that the stereoselection takes place at this stage of the catalytic cycle. Therefore, the early experiments of Halpern and Brown[2−4] can be considered as a useful illustration of different reactivity of diastereomeric intermediates on one of the stages in a catalytic cycle. However, whether or not the induction of chirality really happened on the stage that has been directly monitored must be studied separately.

Of course, in any catalytic asymmetric reaction, the stereoinduction must proceed via the competition of *R*- and *S*-pathways, i.e., via faster transformation of some intermediate compared to the similar transformation of its diastereomer. However, unfortunately this competition is not necessarily directly observed. Neither can simple qualitative structural considerations help in a proper understanding of the intrinsic mechanisms of stereoselection. On the other hand, with the development of computational chemistry, a careful computational analysis of the multitude of elementary steps becomes available.

We are currently studying the mechanisms of the asymmetric hydrogenation of various enamides with several structurally different chiral Rh complexes.

■ ASSOCIATED CONTENT

Supporting Information

The following file is available free of charge on the ACS Publications website at DOI: 10.1021/acscatal.5b00424.

Experimental procedures, NMR charts, computed energies, Cartesian coordinates of all computed structures (PDF)

■ AUTHOR INFORMATION

Corresponding Authors

*E-mail: igridnev@m.tohoku.ac.jp.

*E-mail: imamoto@faculty.chiba-u.jp.

Notes

The authors declare no competing financial interest.

■ ACKNOWLEDGMENTS

The authors are grateful to Ms. Yumi Horiuchi, Nippon Chemical Industrial Co., Ltd. for the measurement of enantiomeric excesses of the hydrogenation products.

■ REFERENCES

(1) (a) *Catalytic Asymmetric Synthesis*, 3rd ed.; Ojima, I., Ed.; Wiley-VCH: New York, 2010. (b) Walsh, P. J., Kozlowski, M. C. *Fundamentals of Asymmetric Catalysis*; University Science Books: Sausalito, CA, 2009. (c) *New Frontiers in Asymmetric Catalysis*; Mikami, K., Lautens, M., Eds.; Wiley: New York, 2007. (d) *Comprehensive Asymmetric Catalysis*Jacobsen, E. N., Pfaltz, A., Yamamoto, H., Eds.; Springer: Berlin, 1999; Vols. *1*−*3*.

(2) Halpern, J. *Science* **1982**, *217*, 401−407. (b) Halpern, J. In *Asymmetric Synthesis*; Morrison, J. D., Ed., Academic Press: New York, 1985; Vol. *5*, pp 41−69.

(3) Brown, J. M. *Chem. Soc. Rev.* **1993**, *22*, 25−45.

(4) Brown, J. M. In *Comprehensive Asymmetric Catalysis*, Jacobsen, E. N., Pfaltz, A., Yamamoto, H., Eds.; Springer: Berlin, 1999, Vol. *1*, pp 119−162.

(5) Landis, C. R.; Halpern, J. *J. Am. Chem. Soc.* **1987**, *109*, 1746−1754.

(6) Landis, C. R.; Hilfenhaus, P.; Feldgus, S. *J. Am. Chem. Soc.* **1999**, *121*, 8741−8754.

(7) Landis, C. R.; Feldgus, S. *Angew. Chem., Int. Ed.* **2000**, *39*, 2863−2866.

(8) Feldgus, S.; Landis, C. R. *J. Am. Chem. Soc.* **2000**, *122*, 12714−12727.

(9) Feldgus, S.; Landis, C. R. *Organometallics* **2001**, *20*, 2374−2386.

(10) Gridnev, I. D.; Higashi, N.; Asakura, K.; Imamoto, T. *J. Am. Chem. Soc.* **2000**, *122*, 7183−7194.

(11) (a) Gridnev, I. D.; Higashi, N.; Imamoto, T. *J. Am. Chem. Soc.* **2000**, *122*, 10486−10487. (b) Gridnev, I. D.; Yasutake, M.; Higashi, N.; Imamoto, T. *J. Am. Chem. Soc.* **2001**, *123*, 5268−5276.

(12) (a) Giernoth, R.; Heinrich, H.; Adams, N. J.; Deeth, R. J.; Bargon, J.; Brown, J. M. *J. Am. Chem. Soc.* **2000**, *122*, 12381−12382. (b) Heinrich, H.; Giernoth, R.; Bargon, J.; Brown, J. M. *Chem. Commun.* **2001**, 1296−1297.

(13) Yasutake, M.; Gridnev, I. D.; Higashi, N.; Imamoto, T. *Org. Lett.* **2001**, *3*, 1701−1704.

(14) (a) Gridnev, I. D.; Higashi, N.; Imamoto, T. *J. Am. Chem. Soc.* **2001**, *123*, 4631−4632. (b) Gridnev, I. D.; Yasutake, M.; Imamoto, T.; Beletskaya, I. P. *Proc. Natl. Acad. Sci. U. S. A.* **2004**, *101*, 5385−5390.

(15) Gridnev, I. D.; Imamoto, T.; Hoge, G.; Kouchi, M.; Takahashi, H. *J. Am. Chem. Soc.* **2008**, *130*, 2560−2572.

(16) (a) Gridnev, I. D.; Fan, C.; Pringle, P. *Chem. Commun.* **2007**, 1319−1321. (b) Gridnev, I. D.; Alberico, E.; Gladiali, S. *Chem. Commun.* **2012**, *48*, 2186−2188.

(17) (a) Gridnev, I. D.; Imamoto, T. *Acc. Chem. Res.* **2004**, *37*, 633−644. (b) Gridnev, I. D.; Imamoto, T. *Chem. Commun.* **2009**, 7447−7464.

(18) Imamoto, T.; Tamura, K.; Zhang, Z.; Horiuchi, Y.; Sugiya, M.; Yoshida, K.; Yanagisawa, A.; Gridnev, I. D. *J. Am. Chem. Soc.* **2012**, *134*, 1754−1769.

(19) Gridnev, I. D.; Kohrt, C.; Liu, Y. *Dalton Trans.* **2014**, *43*, 1785−1790.

(20) Gridnev, I. D.; Liu, Y.; Imamoto, T. *ACS Catal.* **2014**, *4*, 203−219.

(21) Evans, D.; Michael, F. E.; Tedrow, J. S.; Campos, K. R. *J. Am. Chem. Soc.* **2003**, *125*, 3534.

(22) Drexler, H.-J; Baumann, W.; Schmidt, T.; Zhang, S.; Sun, A.; Spannenberg, A.; Fischer, C.; Buschmann, H.; Heller, D. *Angew. Chem., Int. Ed.* **2005**, *44*, 1184.

(23) For recent discussion of the state-of-art computational modelling of enantioselective catalysts, see Armstrong, A.; Boto, R. A.; Dingwell, P.; Contreras-Garcia, J.; Harvey, M. J.; Mason, N. J.; Rzepa, H. S. *Chem. Sci.* **2014**, *5*, 2057−2071.

DOI: 10.1021/acscatal.5b00424
ACS Catal. 2015, 5, 2911−2915